Dried-bakery waste as a substrate for *n*-caproate and *n*-caprylate production *via* chain elongation: bakeroate

*Jean Népomuscène Ntihuga[a], Joseph G. Usack[a,b], Raphael Mayer[a], Ahmed A. Kinbokun[a], Hatice Yesil[a,c], Mei Zhou[a], and Largus T. Angenent[a,d,e,f,g]**

[a]Environmental Biotechnology Group, Department of Geosciences, University of Tübingen, Schnarrenbergstraße 94-96, 72076 Tübingen, Germany

[b]College of Agricultural & Environmental Sciences, University of Georgia, 100 Cedar Street, Athens, GA 30602, USA

[c]Department of Environmental Engineering, Marmara University Maltepe, 34854, Istanbul, Turkiye.

[d]AG Angenent, Max Planck Institute for Biology, Max Planck Ring 5, D-72076 Tübingen, Germany

[e]Department of Biological and Chemical Engineering, Aarhus University, Gustav Wieds vej 10D, 8000 Aarhus C, Denmark

[f]The Novo Nordisk Foundation CO_2 Research Center (CORC), Aarhus University, Gustav Wieds vej 10C, 8000 Aarhus C, Denmark

[g]Cluster of Excellence – Controlling Microbes to Fight Infections, University of Tübingen, Auf der Morgenstelle 28, 72074 Tübingen, Germany

*l.angenent@uni-tuebingen.de

KEYWORDS: Bakery waste; *Bacillus coagulans*; chain elongation; open culture; pertraction; *n*-caproate

ABSTRACT

Bakery waste is a promising feedstock for the circular economy; however, its use for producing medium-chain carboxylates (MCCs) *via* microbial chain elongation remains unexplored. This study investigated pretreatment, pertraction, and chain elongation strategies to convert bakery waste into *n*-caproate and *n*-caprylate. Bakery waste was mechanically and enzymatically processed, and different inocula were tested to optimize the conversion of the resulting glucose-rich solution into lactate and ethanol (intermediates). These intermediates were fed into continuous chain elongation systems, which operated for over 386 days at 37°C and pH 5.5. Results showed that 30–35% of bakery waste carbon was converted into *n*-caproate and 10–15% into *n*-caprylate. Enzymatic starch hydrolysis proved essential, and lactate was a superior intermediate for chain elongation compared to ethanol. A maximum volumetric MCC production rate of 131 mM C L^{-1} d^{-1} (0.1 g L^{-1} h^{-1}) was achieved. This integrated approach, named "bakeraote," demonstrates an efficient pathway for valorizing bakery waste.

1. Introduction

The growing global human population has led to an increased demand for food. The rise in food production and wasteful consumer behaviour has also led to more food-related waste, especially from perishable and semi-perishable products. The imbalance between food production locations and waste generation has become an essential obstacle to food sustainability, resource efficiency, and preservation. A Food and Agriculture Organization (FAO) study revealed that approximately 1.3 billion tons of food waste are produced annually worldwide, equating to the release of 4.4 gigatons of CO_2-eq into the environment and a financial loss of nearly $990 billion (Kim, B. C. *et al.*, 2021). In many countries, short shelf-life and staple food products, such as bread, contribute considerably to food waste (Kumar *et al.*, 2023). For instance, Europe alone produced 3.5 million tons of bakery waste in 2015, with 1.7 million tons originating from Germany (Borrull, 2015).

The optimal solution to reduce bakery waste includes addressing its sources and introducing best waste management practice policies (Brancoli *et al.*, 2020). However, predicting consumer attitudes within the bakery-waste supply chain poses a challenge. Therefore, bakery waste will remain a problem. Fortunately, bakery waste represents an essential source of carbohydrates and substrates for waste valorization platforms that aim to produce valuable chemicals or bioenergy. Previous studies have shown that including bakery waste into bio-based waste management systems can result in the production of biochemicals *(e.g.,* 5-hydroxymethyl-2-furfurylamine), bioenergy (*e.g.,* ethanol and methane), and animal feed through microbial

57 processes, which revalues this waste and reduces its environmental impact (Jung *et al.*, 2022;
58 Narisetty *et al.*, 2022; Gao *et al.*, 2023; Swetha *et al.*, 2023). Despite technological
59 advancements, many bio-based management systems rely mainly on governmental subsidies
60 due to the product's limited commercial value (*e.g.,* methane, ethanol). Consequently, there is
61 a pressing need for a biotechnological platform that transforms bakery waste into more
62 valuable chemicals such as *n*-caproate (4–6 $/kg) and *n*-caprylate (6–8 $/kg) (Debergh *et al.*,
63 2022).

64 Microbial chain elongation is a carbon recovery and production platform that converts
65 complex organic waste into medium-chain carboxylates (MCCs) (*i.e., n*-caproate, *n*-caprylate)
66 as valuable chemicals. This process involves converting short-chain carboxylates (SCCs) and
67 alcohols into MCCs through anaerobic fermentation with cooperative interactions between
68 microbial populations in a food web. Demonstrated examples have highlighted the robustness
69 of chain elongation in revalorizing organic residues, including acid whey (Xu *et al.*, 2019),
70 wastewater (Wu *et al.*, 2020), food waste (Huo *et al.*, 2024), municipal solid waste
71 (Grootscholten *et al.*, 2014), and gas substrates (Quintela *et al.*, 2024). During fermentation,
72 typical metabolic processes break down organic polymers into oligomers, which can be further
73 fermented into chain elongation intermediates, namely lactate and ethanol. These
74 intermediates are subsequently converted into MCCs through reverse ß-oxidation (Angenent
75 *et al.*, 2016). Bakery waste stands out as a highly promising substrate for microbial chain
76 elongation due to its carbohydrate content, which can be converted into lactate and ethanol,

77 and its proteins and amino acids, which can be taken as nitrogen sources for microbial growth.
78 Moreover, using bakery waste for microbial chain elongation offers several advantages,
79 yielding more valuable chemicals (*e.g.*, *n*-caproate) than traditional management systems,
80 which produce methane *via* anaerobic digestion (Battista *et al.*, 2024).

81 Despite the high biotechnological potential of bakery waste as a substrate for microbial chain
82 elongation, there have been no studies with this focus. Previous reports on chain elongation
83 have focused on using other food wastes such as fruits, vegetables, and kitchen waste (Nzeteu
84 *et al.*, 2018; Contreras-Dávila *et al.*, 2020; Kim, H. *et al.*, 2022; Wang *et al.*, 2022). Therefore,
85 exploring bakery waste as a substrate for microbial chain elongation presents an opportunity
86 to establish a sustainable and efficient platform.

87 The bakery-waste starch must be fully hydrolyzed into simple sugars before being used as a
88 microbial chain elongation substrate, because most chain elongating bacteria cannot degrade
89 macromolecules (Li *et al.*, 2024). In addition, when the bakery waste starch is incompletely
90 hydrolyzed, high levels of dextrin are formed, which result in a sticky mass (Every *et al.*, 1996).
91 The stickiness of bakery waste may also be due to damaged starch (Teobaldi *et al.*, 2024).
92 Therefore, careful pretreatment is required to avoid building up the sticky mass on the
93 bioreactor walls and in the tubing due to the presence of the products, as mentioned above.

94 This study explored the potential of using bakery waste in a chain-elongation-production
95 platform as a strategy for carbon recovery and waste management. The main areas of focus
96 included: **(a)** evaluating and optimizing the conversion of bakery waste into chain-elongation

97 intermediates; **(b)** evaluating the feasibility of using bakery-waste mash of different solid
98 content in hollow-fiber membrane extraction applications; and **(c)** producing *n*-caproate and
99 *n*-caprylate. The results of this study are intended to support the integration of organic wastes,
100 particularly those with high carbohydrate content, into a biorefinery concept to produce
101 higher-value products compared to typical waste management strategies.

102 2. Materials and Methods

103 We summarized the experimental methods in the main text. The electronic supplementary
104 information (ESI) contains additional information on experimental parameters, methods, and
105 results. We divided the conversion of bakery waste into the overall process flow into three
106 steps: **(1)** the bakery waste pretreatment, which included bakery waste collection, transport,
107 drying, size reduction, and hydrolysis; **(2)** the conversion of bakery waste into lactate/ethanol
108 for subsequent chain elongation, which included optimizing lactate/ethanol production; and
109 **(3)** the chain elongation process (**Fig. S1,** ESI †). Equations for calculating parameters are also
110 provided in the ESI † (**Eq. S1-S8** in **Bioreactor equations**).

111 2.1. Pretreatment

112 2.1.1. Bakery-waste pretreatment

113 We collected bakery waste with different chemical compositions (**Table S1,** ESI †) from
114 Bäckerhaus Veit (Tübingen, Germany), which we first mechanically and then enzymatically
115 processed. The mechanical processing included drying in ambient air and grinding with a bread

116 grinder (MAC 100, MAC.PAN snc, Thiene, Italy). We used three grinding options in the bakery-
117 waste grinder to achieve different particle size categories of bakery waste. Then, we measured the
118 particle-size distribution of each category using the Mastersizer 2000 (Malvern Instruments
119 Ltd, Worcestershire WR14 1XZ, United Kingdom). As a result, we characterized the ground
120 dried-bakery waste into three categories: **(a)** small-particle dried bakery waste (particle size
121 distribution ≤ 362 μm); **(b)** medium-particle dried bakery waste (particle size distribution
122 between 360 and 680 μm); and **(c)** large-particle dried bakery waste (particle size distribution
123 ≥ 680 μm). The enzymatic processing included liquefaction and saccharification in the
124 Braumeister 20 L (Speidel Tank- und Behälterbau GmbH, Ofterdingen, Germany) using
125 Amylase Thermo and Glucoamylase AN (*Aspergillus niger)* to convert the starch from the
126 bakery-waste mash (8% w/v) into simple sugars. We performed gelatinization, liquefaction,
127 and saccharification according to the enzyme manufacturer's recommendations (ASA
128 Spezialenzyme GmbH, Wolfenbüttel, Germany), resulting in small-particle mash, medium-
129 particle mash, and large-particle mash.

130 **2.1.2. Lactate and ethanol production and optimization**

131 We first optimized lactate and ethanol production considering the following: **(a)** mash
132 pretreatment (small-particle mash, medium-particle mash, and large-particle mash); **(b)**
133 temperature (25˚C, 37˚C, and 50˚C); and **(c)** inoculum type. For the inoculum, we utilized three
134 types: **(1)** a lactate microbiome, which is an inoculum containing *Lactobacillus* sp. with > 98%
135 relative abundance (Schuetterle *et al.*, 2024); **(2)** SiloSolve MC (microbial control), which is a

136 commercial product and a mixture of *Lactobacillus plantarum* (CH 6072), *Enterococcus*
137 *faecium* (DSM 22502), and *Lactococcus lactis* (SR3.54); and **(3)** *Bacillus coagulans* (DSM1). The
138 bacterial culture *B. coagulans* DSM1 strain was procured from the German Collection of
139 Microorganisms and Cell Cultures GmbH (DSMZ, Deutsche Sammlung von Mikroorganismen
140 und Zellkulturen GmbH, Braunschweig, Germany) (**Fig. S1**, ESI †). We directly inoculated
141 the first two inocula mentioned into a continuously-fed 1-L bioreactor (Klask *et al.*, 2020) and
142 pre-cultured the third inoculum on tryptone soya medium (**Tryptone soya medium**, ESI †) at
143 a pH of 7.0 and a temperature of 50°C. For ethanol production, we used the technical yeast
144 Kornbrand, referred to here as yeast (C. Schliessmann Kellerei-Chemie GmbH & Co. KG,
145 Schwäbisch Hall, Germany). After optimizing lactate and ethanol production, we prepared 25
146 L of the small-particle fermented mash in batches and then mixed them to get a total volume
147 of 1000 L for lactate and ethanol product (**Lactate and ethanol preparations**, ESI †). We stored
148 the small-particle fermented mashes at -20°C until usage.

149 **2.2 Chain elongation process**

150 **2.2.1. Feasibility of using bakery-waste mash in liquid-liquid extraction in the chain**
151 **elongation process**

152 The extraction system is described in detail in the ESI † (**Description of extraction system**).
153 Before operating the chain elongation system, which includes in-line extraction, we tested the
154 feasibility of mash in membrane-based liquid-liquid extraction (*i.e.*, pertraction) for the chain

155 elongation process to ascertain its compatibility with this extraction system. We constructed
156 a pertraction system that mimics the experimental setup of the chain elongation system (**Fig.**
157 **S2,** ESI †). We first established a cake during a 12-h fouling experiment for the three different
158 mashes by pushing each mash through the hollow-fiber membrane with a pump (raffinate rate
159 was not constant) at a pressure of 0.6-0.9 bar. Subsequently, we performed a 12-h extraction
160 experiment by connecting the fouled hollow-fiber membranes to the synthetic fermentation
161 broth and the solvent in the same manner as the conventional pertraction system, which uses
162 diffusion of undissociated carboxylic acids rather than pushing a liquid through the
163 membrane. We circulated each of the three mashes, which were enriched with 10 g L^{-1} of *n*-
164 caproate, through the shell side and the solvent through the lumen of the fiber at a flow rate
165 of 2.2 L h^{-1} and 4.3 L h^{-1}, respectively. We maintained a pressure of 0.5 bar on the shell side
166 and 0.2 bar on the lumen side at a temperature of 37°C. We measured the extracted *n*-caproate
167 in the solvent by weighing the solvent at the end of each batch (12 h), assuming that only *n*-
168 caproate diffused. However, we needed to correct for the solvent that remained in the lumen
169 by measuring the solvent reference weight. To measure the solvent reference weight, we first
170 weighed the solvent before adding it to the lumen. Then, we circulated water on the shell side
171 and the solvent for 2, 4, 6, 8, 10, and 12 h before weighing the solvent (six times) (**Batch**
172 **extraction calculations,** ESI†). We successfully verified our approach by connecting the
173 extraction system to a stripping system and measuring the *n*-caproate concentration in the
174 stripping solutions (**Fig. S2**, ESI†).

175 **2.2.2. Chain elongation bioreactor system**

176 We added yeast extract (1.25 g L^{-1}) and trace elements to the small-particle fermented mash
177 before feeding to the bioreactors, but without vitamins and minerals (**Bioreactor medium**
178 **preparation**, ESI†) (Rajagopalan *et al.*, 2002; Vasudevan *et al.*, 2014; Kucek *et al.*, 2016; Spirito
179 *et al.*, 2018). In addition, we added hydrochloric acid or sodium hydroxide to adjust the pH
180 between 5.0 and 5.4. Depending on the operating period, we added tap water to dilute the
181 small-particle fermented mash, and referred to the solutions as lactate medium or ethanol
182 medium. We set up two independently, identically, and continuously fed upflow bioreactors
183 with fermentation-broth recirculation through both a direct route and through a pertraction
184 system (**Fig. 1**). One bioreactor was fed with lactate medium and the other bioreactor with
185 ethanol medium. We used a peristaltic pump (Model 07528-20, Cole Parmer) to continuously
186 supply fresh medium at room temperature from a 5-L medium tank to each bioreactor. This
187 medium tank was flushed with nitrogen gas. We used peristaltic pumps (Model 7528-30, Cole-
188 Parmer, Vernon Hills, IL, USA) to recirculate the fermentation broth through a pertraction
189 system (**Description of extraction system,** ESI †). Each bioreactor was connected to an
190 automated thermostat (CC 104A, Huber, Raleigh, NC, USA), which controlled the
191 fermentation-broth temperature at 37°C for lactate and 30°C for ethanol (**Table S2,** ESI †). The
192 extraction systems for each bioreactor were controlled at the same temperature as the
193 fermentation broth. We placed the pH electrode (ProcessLine 80-325pH, SI Analytics,
194 Weilheim, Germany) through the lid of the bioreactor and connected it to a pH controller

(Bluelab pH controller, Bluelab Corporation Limited, Tauranga, New Zealand). The controller maintained the pH at 5.5 by adding hydrochloric acid (3 M).

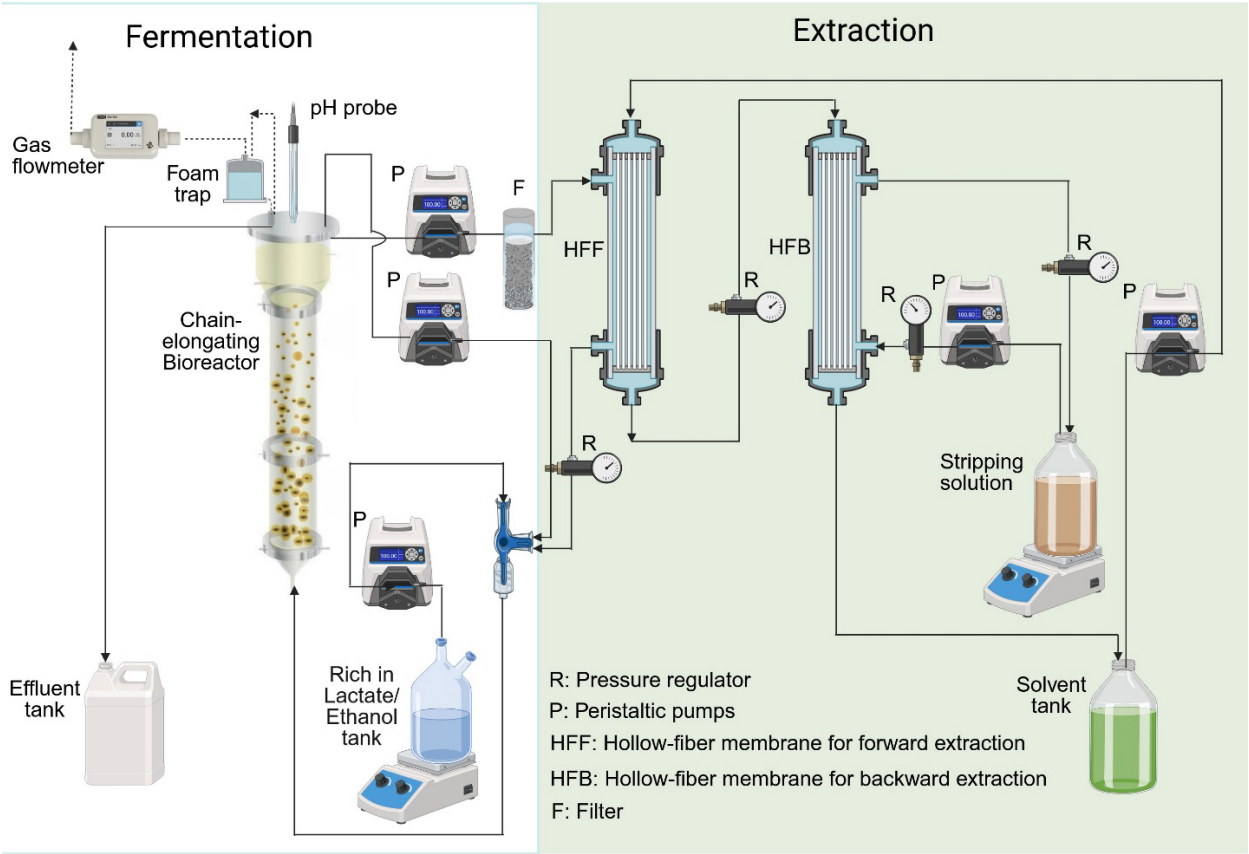

Figure 1. Chain elongation step, including bioconversion and product extraction (step 3 in the overall process flow of the bakery-waste conversion system).

2.2.3. Chain elongation system operating periods

We divided the operating periods into Periods 0-2. An operating period of 92 days (**Period 0**) (data not shown) was initiated to learn how to perform start-up (**Table S2,** ESI †). First, we tested different anaerobic digester sludges to ascertain the preferred inoculum. We compared three different inocula: **(1)** sludge from an anaerobic digester treating manure; **(2)** sludge from

205 an anaerobic digester treating waste-activated sludge; and **(3)** a combination of these two
206 inocula (1:1). Each sludge passed through an 0.6-mm screen mesh to remove large particles.
207 Second, for the combination of the inocula (the preferred inoculum), we determined the ideal
208 operating parameters for the start-up period: hydraulic retention time (HRT); the recycling
209 flow rate of the fermentation broth; the flow direction of the fermentation broth; the
210 hydrophobic solvent in forward and backward membrane contactors; and the substrate
211 concentration to start with (**Table S2,** ESI †).

212 We indicated the first reported day as Day 1 during **Period 1** (Day 1–44). During this operating
213 period, we wanted to reach a recommended volumetric production rate of caproate >60 mmol
214 C L^{-1} d^{-1} as fast as possible (Kim, B. C. *et al.*, 2021). Therefore, we added the electron acceptor
215 *n*-butyrate to the electron donor lactate at final concentrations of 50 mM and 160 mM,
216 respectively. Similarly, acetate was added to ethanol at final concentration of 50 mM and 150
217 mM, respectively. After we reached the targeted *n*-caproate volumetric production rates, we
218 stopped the external supply of electron acceptors for both bioreactor systems during **Period 2**
219 (Day 44–386). For the lactate medium, we increased the lactate concentration in increments
220 of 25 mM after every 2 HRTs from 160 mM to 260 mM by reducing the dilution with tap
221 water. For the ethanol medium, we used increments of 25 mM to increase the ethanol
222 concentration from 150 mM to 190 mM. During these operating periods, we maintained the
223 systems' anaerobic conditions because a peristaltic pump connected to a time switch pulsed

224 the reducing agent solution (3M Na_2S) periodically into the recycling flow of the fermentation
225 broth for each bioreactor system. The pump was on 1 min every 3 h, totaling 8 min d^{-1}.

226 **2.3. Analytical procedures and calculations**

227 During the pretreatment step, after collecting and drying the bakery waste, we first analyzed
228 the starch content of the dried bakery waste using the rapid total starch (RTS) and the rapid
229 total starch NaOH (RTS-NaOH) method (Total Starch [AA/AMG]) Assay Kit 2020,
230 amyloglucosidase/alpha-amylase method, Neogen, Michigan, US). Then, in the conversion
231 steps, we used high-performance liquid chromatography (HPLC) (Shimadzu, Kyoto, Japan) to
232 measure lactate, ethanol, and simple sugars. We used the total organic carbon (TOC) method
233 (TOC-LCPN FA, E200, Shimadzu, Kyoto, Japan) to measure the carbon content of
234 unmetabolized and unknown compounds. For the chain elongation step, we first collected 2
235 mL of liquid samples from the bioreactors' fermentation broth and alkaline extraction solution
236 daily (at the beginning) and twice a week afterwards. The fermentation broth samples were
237 taken from a sampling port at the top of the bioreactors and were divided into two parts: **(a)**
238 for immediate measurement of total ammoniacal nitrogen (*i.e.*, both the free ammonia (NH_3)
239 and ammonium salt (NH_4^+) in NH_4^+-N); and we calculated the free ammonia based on **Eq. S7**
240 (ESI†); and **(b)** for the measurement of MCCs in effluent. To collect alkaline-extraction
241 solution samples, we provided a T-shaped sampling adaptor in the recirculation line between
242 the reservoir tank exit and the backward membrane contactor. We stored all the liquid samples
243 in 1.5-mL Eppendorf tubes at -20°C until analysis. Next, we collected and immediately

244 measured the gas samples twice a week at the gas sampling port between the top of the
245 bioreactors and the gas flow measuring equipment (Ritter MilliGascounter, Dr.-Ing. Ritter
246 Apparatebau GmbH & Co.KG, Bochum, Germany).

247 We used an Agilent 7890B gas chromatograph (GC) (Agilent Technologies Inc., Santa Clara,
248 CA, USA) to measure the concentrations of carboxylates (Gemeinhardt *et al.*, 2025) and a gas
249 chromatography (GC-FID) (SRI gas GCs, SRI Instruments, Bad Honnef, Germany) for biogas
250 measurement (Gemeinhardt *et al.*, 2025). We normalized all given values to mmol carbon
251 atoms (mmol C). We developed a volumetric production rate and specificity equations based
252 on previously reported equations to compensate for the dilution of carboxylates in the alkaline
253 extraction solution (**Eq. S8**, ESI†) (Palomo-Briones *et al.*, 2022) and (**Eq. S8,** ESI †**)** (Xu *et al.*,
254 2018), respectively.

255 **3. Results and discussion**

256 **3.1. Optimized pretreatment conditions were determined for lactate and ethanol**
257 **production from dried bakery waste**

258 We converted three different dried bakery wastes based on their size into glucose by
259 enzymatic treatment. The conversion efficiency for the small-particle dried bakery waste (≤
260 362 μm), medium-particle dried bakery waste (between 360 and 680 μm), and large-particle
261 dried bakery waste (≥ 680 μm) into glucose was 98%±0.66%, 62%±0.36%, and 50%±0.25%
262 (triplicate measurement), respectively (**Fig. S3,** ESI †**)**. The results showed that solids-particle

263 size affected the release of glucose from the bakery waste, which might be due to: **(a)** the
264 particle sizes changing the properties of bakery waste, including the total surface area, and
265 therefore affecting substrate-enzyme interaction (Guerra-Oliveira *et al.*, 2022); **(b)** the
266 increasing solid content hindering the substrate-enzyme interaction (Thani *et al.*, 2021); **(c)**
267 the protein matrix affecting the shape and accessibility of starch granules; and **(d)** the
268 increasing protein content resulting in the deformation of the starch structure, making it
269 difficult for the starch to be degraded (Agu *et al.*, 2009). The results showed that the dried
270 bakery waste with small particle sizes is superior. However, small particle sizes could increase
271 the downstream load of the centrifuge. Therefore, the choice of particle size must be a
272 compromise between yield and minimizing problems for the downstream process.

273 The thermodynamic capacities of lactate and ethanol to operate as electron donors for chain
274 elongation are similar (Weimer *et al.*, 2016). Lactate conversion to MCCs releases CO_2, while
275 ethanol conversion does not, because ethanol has an average carbon atom oxidation number
276 that is more reduced than that of lactate. Because of similar thermodynamic capacities, we
277 optimized the conversion of the glucose-rich solution into both lactate and ethanol (**Table S3**,
278 ESI †). For lactate production, the results showed that the small-particle mash that was
279 pretreated with *B. coagulans* DSM1 produced the highest lactate concentration (263±0.120
280 mmol L^{-1}) at a temperature of 50°C compared to the other inoculants (**Table S3**, ESI †). In
281 addition, the large-particle mash that was pretreated with the lactate microbiome performed
282 better than *B. coagulans* and Silosolve MC at low temperatures. For example, at 25°C, the

283 lactate concentrations were 121±41.1, 55.1±10.2, and 45.2 ± 14.2 mmol L^{-1} using the lactate
284 microbiome, *B. coagulans* DSM1, and Silosolve MC, respectively (**Table S3**, ESI †). This might
285 be explained by the fact that the lactate microbiome was an open culture with different
286 microbial populations, which could be active at different temperatures (Schuetterle *et al.*,
287 2024). The disadvantage of using a lactate microbiome was that it produced a mixture of lactate
288 and ethanol, reducing the selectivity for lactate production. Silosolve MC performed worst as
289 an inoculant because it is intended to control fermentation during silage (Daniel *et al.*, 2018).
290 For ethanol, the maximum concentration was 180 ± 0.22 mmol L^{-1} at 30°C, which is the
291 optimum temperature for technical yeast. In general, we observed the same advantage of the
292 smaller particle size in mashes for the lactate and ethanol production compared to the glucose
293 production: small-particle mash > medium-particle mash > large-particle mash (**Fig. S3, Table**
294 **S3,** ESI †). Therefore, for the rest of the microbial chain elongation study, we decided to use:
295 **(a)** the small-particle fermented mash; **(b)** the *B. coagulans* DSM1 inoculum to produce lactate;
296 and **(c)** the technical yeast to produce ethanol.

297 **3.2. The bakery-waste solids reduced the raffinate flux for the extraction system that**
298 **will be coupled to the chain elongation system**

299 As discussed in the introduction, starch-rich substrates can cause stickiness. In addition,
300 particles from bakery waste can also form cakes. Therefore, we performed short-term
301 experiments (24 h) to test how fouling of our hollow-fiber membranes throughout longer
302 operating periods could negatively impact pertraction. Under normal operating conditions,

303 the undissociated *n*-caproic acid diffuses from the fermentation broth to the solvent, and thus
304 no liquid is pushed through the membrane with small holes of around 200 nm. Our 24-h
305 experiment was divided into two sections. First, we fouled the membrane intentionally by
306 pushing the various fermented mash types through our membrane at a constant pump rate for
307 12 h during which we studied the decline in raffinate flux (*i.e.*, the clear liquid). We observed
308 for all fermented mash types that the decline in raffinate flux can be divided into two decay
309 periods: a sharp-decay period (0–2 h) and a pseudo-steady-state-decay period (2–12 h) (**Fig.**
310 **2A**). The reduction in raffinate flux was caused by a constant increase in solids retardation,
311 depositing a cake/gel layer on the hollow-fiber membrane, especially for the large-particle
312 fermented mash (**Fig. 2B**). For the small-particle fermented mash, we still observed a sharp-
313 decay period, albeit not as dramatic as the medium- and large-particle fermented mash types
314 (**Fig. 2A)**, even though the fouling rate was minimal. We do not know why the raffinate flux
315 decreased sharply during the sharp-decay period for the small-particle fermented mash

316 Second, we performed conventional pertraction for 12 h using the hollow-fiber membranes
317 from the three fermented mash types after 12 h during the fouling section. The increasing
318 amounts of formed cake/gel on the surface of the hollow-fiber membranes from the small-,
319 medium, and large-particle fermented mash resulted in an increased resistance during
320 pertraction, leading to a slower extraction rate of undissociated *n*-caproic acid throughout the
321 12-h experimental period of section 2 (**Fig. 2C**). De Sitter *et al.* (2018) found the same
322 observation with different hollow-fiber membrane properties. The effect of bakery-waste solids

323 on the extraction system showed that the small-particle mash performed better than medium-
324 particle and large-particle mashes (**Fig. 2C**). The extraction of *n*-caproate was reduced when
325 the fouling factor of the membrane increased; for example, we extracted 40 mM and 15 mM
326 when the fouling factor was $4x10^{-3}$ mg L^{-1} m^{-2} and 3.75 mg L^{-1} m^{-2}, respectively (**Fig. 2C**).
327 Therefore, we used small-particle bakery-waste mash for the chain elongation experiments to
328 avoid excessive fouling of the membrane for MCC extraction.

329

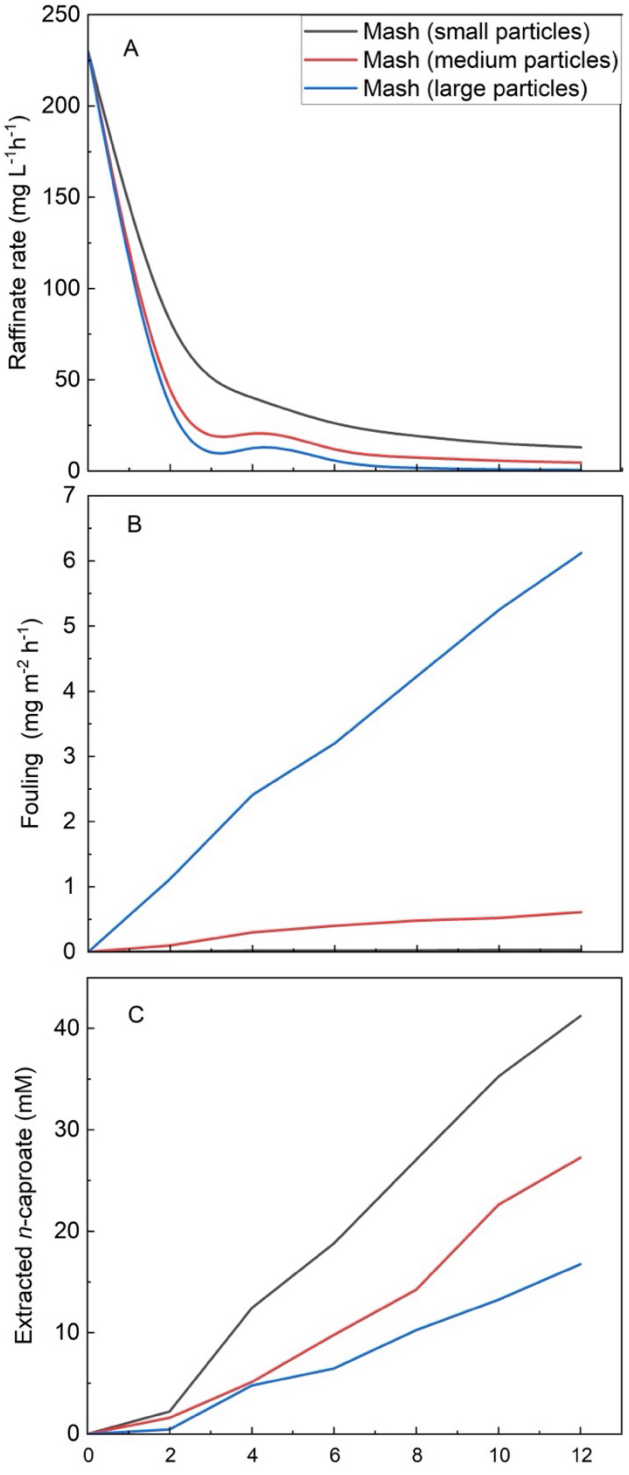

Figure 2. Effect of different fermented mash types on fouling and MCC extraction for the hollow fiber-membrane: **A**) raffinate rate during the 12-h fouling experiment, **B**) fouling effect during the 12-h fouling experiment, and **C**) extracted *n*-caproate during the 12-h extraction experiment.

335 **3.3. Only the chain elongation experiment with the intermediate lactate as the electron**
336 **donor resulted in satisfactory MCC selectivities.**

337 Initially, we intended to use and compare lactate-rich and ethanol-rich substrates to produce
338 MCCs. Unfortunately, the bioreactor fed with an ethanol-rich substrate did not behave as
339 envisioned and produced excessive methane, which is typical for an anaerobic digester. We
340 were unable to improve performance, even during a lengthy operating period, despite
341 implementing several operating optimizations. Possibly, the ratio of ethanol (electron donor)
342 to other substrates (electron acceptor) was too low to produce MCCs, lacking enough reducing
343 power. Therefore, we summarized the results of the bioreactor fed with the ethanol-rich
344 substrate in the supporting information (**Result summary of ethanol-bioreactor, Fig. S4-S5,**
345 ESI †). Here, we focused on the performance and behavior of the chain-elongating bioreactor
346 that was fed with a lactate-rich substrate.

347 **3.3.1. Chain elongation with lactate as the electron donor, with an external *n*-butyrate**
348 **supply, was accelerated**

349 A start-up study with reactor microbiomes achieved increased volumetric *n*-caproate
350 production rates during a short operating period after inoculation with anaerobic digester
351 sludge. They added *n*-butyrate as an electron acceptor, in addition to the electron donor, for
352 chain elongation of different substrates (Kim, B. C. *et al.*, 2021; Nzeteu *et al.*, 2022). Acetate as
353 an alternative electron acceptor would have been a possibility, but Wu *et al.* (2019) showed a

354 low *n*-caproate volumetric production with acetate. Therefore, we shaped the *n*-caproate-
355 producing microbiome by using lactate as the electron donor and by externally adding *n*-
356 butyrate as an electron acceptor, and utilizing a mixed inoculum (**The choice of inoculum,**
357 ESI †). We know from previous studies that feeding primarily electron donors, such as lactate
358 and ethanol, is also possible, but that a lack of growth must be anticipated (Allaart *et al.*, 2024).
359 Therefore, we opted to externally add electron acceptors to speed up the growth and
360 acclimation of the microbiome during the initial start-up period for the chain-elongating
361 bioreactors.

362

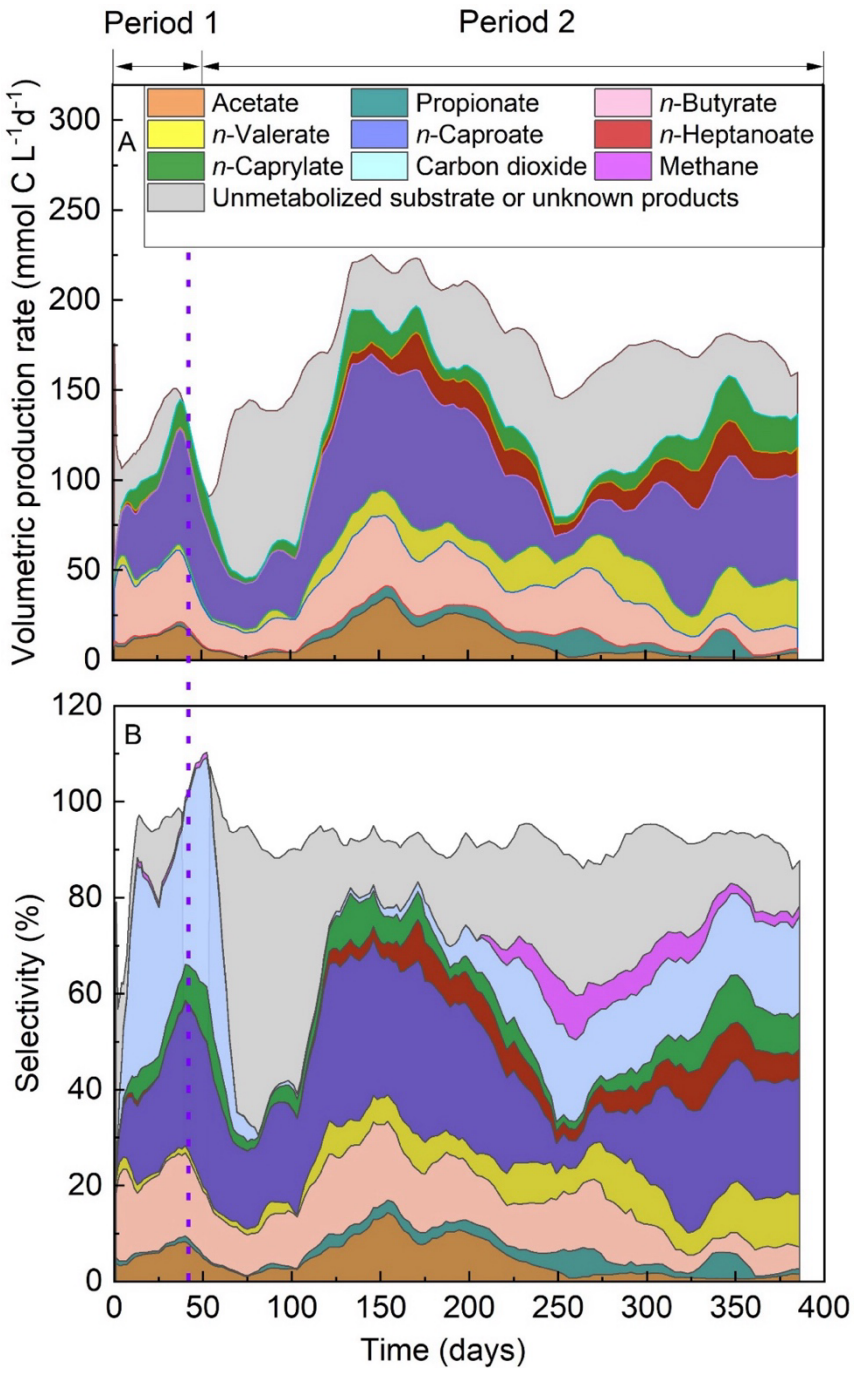

363

364 **Figure 3**. Carboxylate, unmetabolized substrate/unknown product, and gas profiles
365 throughout the operating period from the bioreactor that was fed with lactate as an
366 intermediate after pretreatment of bakery waste: **A**) volumetric production rates, and **B**)
367 selectivity. The volumetric production rates and selectivities were calculated, and the graphs
368 were smoothed with a six-measurement moving average. Operating periods 1 and 2 are
369 indicated and described in the Materials and Methods section.

370 From Day 1 to 44, the volumetric production rates of *n*-caproate and *n*-caprylate increased
371 steadily, reaching 70 mmol C $L^{-1}d^{-1}$ and 18 mmol C $L^{-1}d^{-1}$, respectively (**Fig. 3A**). For *n*-
372 Butyrate, we found a fluctuating volumetric production rate of 38 mmol C $L^{-1}d^{-1}$ and 50 mmol
373 C $L^{-1}d^{-1}$, while the volumetric production rate for acetate reached 22 mmol C $L^{-1}d^{-1}$ (**Fig. 3A**).
374 In addition, the carbon mass balance showed that 30.6% of the carbon fed in the upflow
375 bioreactor ended up in CO_2 production (**Fig. 3B**), which is as anticipated because one carbon
376 atom out of three carbon atoms of lactate is oxidized to CO_2, according to the stoichiometry.
377 Kim, B. C. *et al.* (2021) showed that the addition of *n*-butyrate to lactate as an electron donor
378 quickly (84 h) acclimated the MCC-producing microbiome during bottle experiments (batch-
379 fed, non-open culture). We also found that in a continuously fed open-culture bioreactor, the
380 enrichment of an MCC-producing microbiome progressed rapidly (a couple of days in (**Fig.**
381 **3**)).

382 **3.3.2. More research is necessary to understand whether the external addition of *n*-**
383 **butryate actually shortened the microbiome acclimation period or not.**

384 However, after 44 days, when we removed the externally added *n*-butyrate, because we
385 wanted to only use lactate as the substrate, unstable conditions occurred (broken line on Day
386 44 in **Fig. 3**). The absence of *n*-butyrate led to a large amount of unmetabolized substrate and
387 unknown products (enlarged gray area in **Fig. 3**), and a decrease in the volumetric *n*-caproate
388 production rate from 64.76 to 23.68 mmol C $L^{-1}d^{-1}$ on Day 44 and 90, respectively (**Fig. 3A**).
389 Due to these unstable conditions, we needed an additional acclimation period (**Fig. 3**).

390 Between Days 44 and 129, we observed an increase in the volumetric production rate of odd-
391 number carboxylates, especially *n*-valerate and *n*-heptanoate, which increased 6-fold (**Fig.**
392 **3A**). We also observed a gradual increase in the volumetric *n*-caproate production rates from
393 64.76 mmol C $L^{-1}d^{-1}$ on Day 44 to 81.68 mmol C $L^{-1}d^{-1}$ on Day 129 (**Fig. 3A**). Thus, the combined
394 acclimation periods took 129 days.

395 We hypothesized that circumventing *n*-butyrate led to: (**1**) the disruption of redox balance,
396 leading to a microbial metabolic shift, which caused the production of undesired products and
397 unmetabolized substrate, which resulted in a decrease in SCC production; and (**2**) the
398 degradation of protein into amino acids, contributing to odd-number carboxylate production.
399 Steinbusch *et al.* (2011) state that internal redox balancing and microbial metabolism stability
400 are necessary for the chain elongation process without an electron acceptor. Here, it took
401 approximately another 90 days for redox balancing and microbial metabolism to stabilize after
402 removing the external electron acceptor (**Fig. 3B**). We observed that between Day 75 and Day
403 175, the specificity of CO_2 was close to zero (**Fig. 3B**). This operating period included the
404 acclimating period during which redox balancing must have occurred. We observed an
405 increase in homoacetogenesis (*i.e.*, acetate production) during this period with an excess of
406 reducing equivalents due to the sudden absence of the external electron acceptor from *n*-
407 butyrate, because methane production was still absent (**Fig. 3B**). Indeed, the selectivity of
408 acetate went from 2% to 16% between Day 75 and Day 175 (**Fig. 3B**), explaining why we did
409 not observe CO_2 in headspace as anticipated by the stoichiometry.

410 The maximum volumetric *n*-caproate production rate of 94.2 mmol C $L^{-1}d^{-1}$ (0.08 g L^{-1} h^{-1}) was
411 achieved on Day 175 of the operating period (**Fig. 4A**), which coincided with the maximum
412 *n*-caproate selectivity of 55% (**Fig. 3B**). The acclimation of the microbiome continued with
413 the highest volumetric *n*-valerate (unwanted) and *n*-caprylate (wanted) of 42.8 mmol C $L^{-1}d^{-1}$
414 and 26.8 mmol C $L^{-1}d^{-1}$ being achieved on Day 235 and Day 351, respectively (**Fig. 4A**). A
415 continuous reduction in the performance between Day 175 and Day 248 was due to a faulty
416 pH probe, and the system recovered again after this experimental problem had been mitigated
417 (**Fig. 4A**). A stable maximum average *n*-caprylate specificity of 11.1 ± 6.88% (n=387) was
418 achieved at the end of the operating period during which the maximum average overall MCC
419 specificity was 55.2 ± 14.1 % (n=386; **Fig. 4A**). We would have to perform a side-by-side study
420 to investigate whether the external addition of *n*-butyrate, which looked promising during the
421 first 44 days of the operating period (**Fig. 3B**), compared to the absence of *n*-butyrate would
422 resulted in a different total acclimation period for the microbiome to produce MCCs.

423

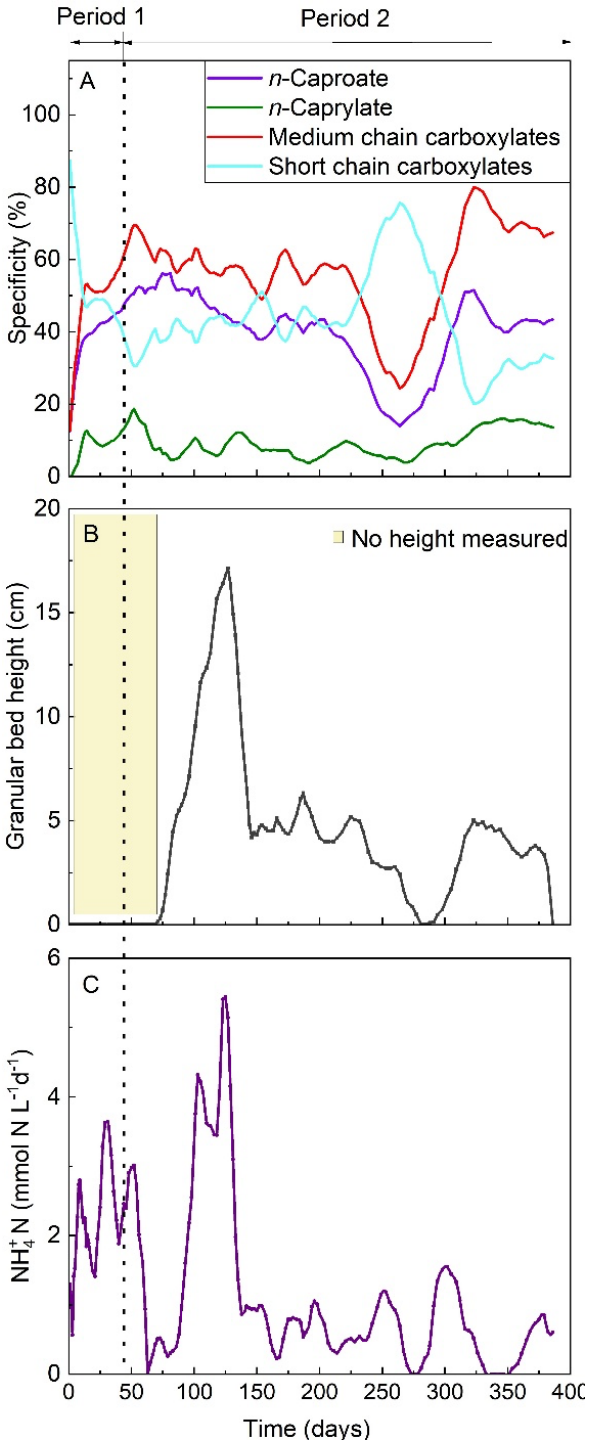

Figure 4. Effect of pseudo-granules and ammonium nitrogen concentrations on the specificities of carboxylates: **A**) specificity of carboxylates, **B**) pseudo-granular bed height in the bioreactor, and **C**) volumetric ammonium nitrogen production rate. The product specificities, pseudo-granular bed heights, and volumetric ammonium nitrogen production rates were calculated, and the graphs were smoothed with a six-measurement moving average.

430 **3.3.3. The lactate-fed chain elongation bioreactor formed pseudo-granules, which were**
431 **not stable**

432 During Period 1, we observed the presence of a few pseudo-granules at the bottom of the
433 bioreactor; however, we had not yet measured the granular bed height in the bioreactor. At
434 the beginning of Period 2, the pseudo-granules grew in numbers, and we started to measure
435 the granular bed height (**Fig. 4B**). The granules were not stable, and we observed several rapid
436 drops in granular bed height, including on Day 133 of the operating period (**Fig. 4B**). This
437 change occurred without changes in the performance (**Fig. 3A-B**), which is why we called
438 them pseudo-granules (**Fig. S6**, ESI †). We were unable to remove the pseudo-granules from
439 the bioreactor to analyze and confirm their nature. Real anaerobic granules remain as
440 individual entities even after sludge settling; however, we could not perform this
441 measurement without disintegrating the pseudo-granules. According to Roghair *et al.* (2016),
442 chain elongation with granular sludge could become a high-rate biotechnological process.
443 However, based on the disintegration of our pseudo-granules, developing a granulation
444 concept around the chain elongation of the dried-bakery waste would not be feasible. In
445 addition, the presence of pseudo-granules had a little impact on volumetric production rate
446 and specificity for *n*-caproate and *n*-caprylate (**Fig. 3A, Fig. 4B**).

447

448

449 **3.3.4. Ammonium-nitrogen production from protein degradation is pertinent as a**
450 **nitrogen source and pH control**

451 The volumetric ammonium-N production rate increased to 2.8 mmol N L^{-1} d^{-1} from Day 0 to
452 Day 18 of the operating period, and then fluctuated between 2.8 mmol $NL^{-1}d^{-1}$ and 3.9 mmol
453 N L^{-1} d^{-1} until Day 44 (**Fig. 4C**). A lower biological activity after removing the external *n*-
454 butyrate addition on Day 44 resulted in a considerably reduced volumetric ammonium-N
455 production rate (**Fig. 4C**). The acclimation of biomass due to pseudo-granulation occurred
456 after the removal of external *n*-butyrate, and was likely not due to the changes in ammonium-
457 N concentrations. The pseudo-granulation on Day 74 started before a renewed sharp increase
458 in the ammonium-N concentration on Day 83. In addition, during Period I, no pseudo-
459 granules were observed even though a relatively high concentration of ammonium-N was
460 achieved (**Fig. 4B**, **Fig. 4C**).

461 From Day 62 to Day 125, the volumetric ammonium-N production rate increased sharply with
462 a maximum of 5.6 mmol N L^{-1} d^{-1} on Day 127 of the operating period (**Fig. 4C**). We observed
463 a sharp decline after which the volumetric ammonium-N production rate fluctuated, but
464 remained below 1 mmol N L^{-1} d^{-1} until Day 386 (**Fig 4C**). We do not understand why we
465 observed these fluctuations. We speculate an interplay between the following: **(1)** protein
466 decomposition to produce ammonium-N; **(2)** fluctuation of the incoming protein
467 concentration in the lactate-rich substrate; **(3)** fluctuations in operating parameters (*e.g.*, cell
468 optical density, pH, and temperature); and **(4)** removal of ammonium-N due to biomass

469 growth. We also observed a variation in the concentration of ammonium-N along the effective
470 height of the bioreactor (data not shown). The latter variation could be the result of varying
471 biomass concentrations along the effective height of the bioreactor. However, the fluctuations
472 of the volumetric ammonium-N production rates had little impact on the volumetric
473 production rate of *n*-caproate and *n*-caprylate (**Fig. 3A, Fig. 4C**).

474 **3.3.5. Sankey diagram for bakery waste conversion *via* microbial chain elongation**

475 The Sankey diagram with the carbon flow in our bakery-waste fermentation system provides a
476 summary and clear visual representation of microbial chain elongation with (**Fig. 5A**) and without
477 (**Fig. 5B**) *n*-butyrate as the external electron acceptor. We normalized all measured values of
478 TOC in bakery waste to 100 kg of carbon atoms (kg C), which represented 143 kg of dried
479 bakery waste. The microbial chain-elongation of bakery waste with *n*-butyrate as an externally
480 added eletron acceptor resulted in the wanted products of 20.1 kg C of *n*-caproate and 4.74 kg C
481 of *n*-caprylate, while the co-products consisted of: 0.490 kg C of *n*-heptanoate; 26.5 kg C of SCCs;
482 32.0 kg C of CO_2; 0.977 kg C of CH_4; and 32.9 kg C of unmetabolized substrate or unknown
483 products (**Fig. 5A**). The microbial chain elongation without *n*-butyrate addition resulted in 22.1
484 kg C of *n*-caproate and 5.00 kg C of *n*-caprylate as wanted product, which is slightly higher but
485 not that different from when *n*-butyrate was added. However, in this representation, which was
486 based on 100 kg of bakery waste, we did not account for the kg of C in the added *n*-butyrate. For
487 without *n*-butyrate, the co-products were: 4.20 kg C of *n*-heptanoate; 23.1 kg C of SCCs, 10.1 kg
488 C of CO_2, 2.21 kg C of CH_4, and 32.4 kg C of unmetabolized substrate or unknown products (**Fig.
489 5B**). The difference between with and without *n*-butyrate was mostly in the reduced selectivity of

CO_2. We hypothesize that without *n*-butyrate, the microbiome is forced to produce its own electron acceptor, acetate, through acetogenesis, thereby reducing the amount of CO_2 in the bioreactor's headspace.

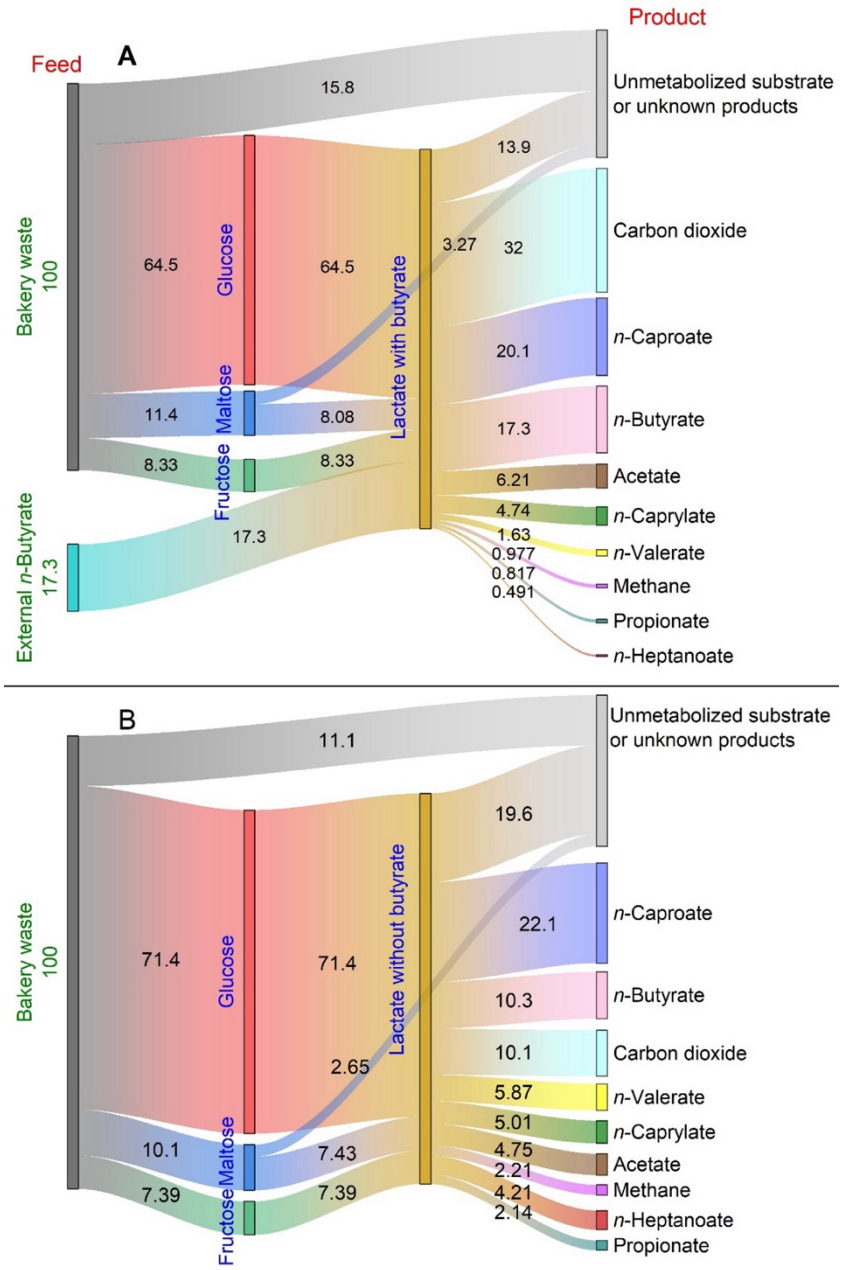

Figure 5. Sankey diagram for bakery-waste conversion *via* pretreatment steps and microbial chain elongation: **A**) chain elongation with the supply of external *n*-butyrate, and **B**) chain elongation without the supply of external *n*-butyrate (unit is kg C).

497 The carbon of unmetabolized or unknown products included the carbon lost during the size
498 reduction in the bakery waste. Clearly, there is a need for improvement to recover residual carbon
499 (unmetabolized substrate and unknown products) (**Fig. 5A, Fig. 5B**). Nevertheless, we achieved a
500 higher carbon conversion to *n*-caproate and *n*-caprylate compared to food wastes in other studies.
501 For example, Huo *et al.* (2024) in their chain elongation study, the conversion from food waste
502 carbon to *n*-caproate was 15.5%, with no carbon converted to *n*-caprylate. Therefore, our study is
503 among the few studies that have converted food waste that is rich in carbohydrates into *n*-caprylate
504 using continuous chain elongation coupled with pertraction.

505 **4. Conclusions**

506 We investigated the recovery of carbon in bakery waste by first converting it into the
507 intermediate lactate, which was then utilized as an electron donor for the microbial chain
508 elongation process to produce medium-chain carboxylates. We achieved a satisfactory
509 medium-chain carboxylate production rate for lactate as an electron donor. However, our
510 efforts with ethanol as an intermediate did not result in a satisfactory production rate. Our
511 results identified that the chain elongation process with lactate, when coupled to pertraction,
512 required: **(a)** the filtration of bakery-waste mash to avoid fouling of the membrane,
513 consequently optimizing pertraction; **(b)** a mash containing solid particles with an average size
514 distribution of ≤ 362 μm; and **(c)** *Bacillus coagulans* DSM1 inoculum to produce lactate
515 effectively. The bakery waste mash with small particle sizes was the best for pretreatment and
516 pertraction. However, small particle sizes might increase the centrifuge load in large-scale
517 applications. Thus, the choice of particle size must be a compromise between yield and

minimizing problems in the downstream process. The results of this study inspire the development of bakery waste pretreatment, chain elongation, and product recovery strategies for *n*-caproate and *n*-caprylate production, as well as the conversion of the processing system's residual solids into methane. We refer to this process as the bakaroate process.

CRediT authorship contribution statement

Jean Népomuscène Ntihuga: Conceptualization, data curation, formal analysis, investigation, methodology, project administration, visualization, writing-origin draft, writing-review & editing. **Joseph G. Usack:** Conceptualization, project administration, supervision, writing-review & editing, **Rafael Mayer:** data curation, writing-review & editing. **Ahmed K. Kinbokun:** data curation, writing-review & editing. **Hatice Yasil:** data curation, writing-review & editing. **Mei Zhou:** data curation, writing-review & editing. **Largus T Angenent:** Conceptualization, funding acquisition, project administration, resources, supervision, and writing-review & editing

Declaration of competing interest

Lars Angenent has ownership in a start-up company specializing in medium-chain carboxylic acid production, which is known as Capro-X, Inc.

Acknowledgments

Largus T. Angenent acknowledges the support from the Alexander von Humboldt Foundation within the framework of the Alexander von Humboldt Professorship, which is endowed by the Federal Ministry of Education and Research in Germany. The authors acknowledge the support of Bäckerhaus Veit for providing the bakery waste at no cost. We thank Abha Mansoor and Fady Isaac from the University of Tübingen for their support in operating the bioreactors. Finally, we thank a group of M.Sc. students, consisting of Chenhui Chang, Chih-Fu Cheng, and Elena Schiller, for their contribution to the ideation process.

References

Agu, R. C., Swanston, J. S., Walker, J. W., Pearson, S. Y., Bringhurst, T. A., Brosnan, J. M., *et al.* (2009). Predicting alcohol yield from UK soft winter wheat for grain distilling: Combined influence of hardness and nitrogen measurements. *Journal of the Institute of Brewing, 115*(3), 183-190.

Allaart, M. T., Fox, B. B., Nettersheim, I. H. M. S., Pabst, M., Sousa, D. Z., & Kleerebezem, R. (2024). Physiological and stoichiometric characterization of ethanol-based chain elongation in the absence of short-chain carboxylic acids (vol 13, 17370, 2023). *Scientific Reports, 14*(1).

553 Angenent, L. T., Richter, H., Buckel, W., Spirito, C. M., Steinbusch, K. J. J., Plugge, C. M., *et*
554 *al*. (2016). Chain Elongation with reactor microbiomes: Open-culture biotechnology to
555 produce biochemicals. *Environmental Science & Technology, 50*(6), 2796-2810.
556 Battista, F., & Bolzonella, D. (2024). Beyond anaerobic digestion: New perspectives for the
557 development of a biorefinery platform for the simultaneous production of medium-
558 chain fatty acids by chain elongation and biogas from food wastes. *Acs Sustainable*
559 *Chemistry & Engineering, 12*(42), 15294-15306.
560 Borrull, R. G. (2015). *BREAD4PLA:* Demonstration - plant project to produce poly-lactic acid
561 (PLA) biopolymer from waste products of bakery industry. Retrieved from Valencia:
562 http://ec.europa.eu/environment/life/project/Projects/index.cfm?fuseaction=search.ds
563 pPage&n_proj_id=3996#PD
564 Brancoli, P., Bolton, K., & Eriksson, M. (2020). Environmental impacts of waste management
565 and valorisation pathways for surplus bread in Sweden. *Waste Management, 117*, 136-
566 145.
567 Contreras-Dávila, C. A., Carrión, V. J., Vonk, V. R., Buisman, C. N. J., & Strik, D. P. B. T. B.
568 (2020). Consecutive lactate formation and chain elongation to reduce exogenous
569 chemicals input in repeated-batch food waste fermentation. *Water Research, 169*.
570 Daniel, J. L. P., Queiroz, O. C. M., Arriola, K. G., Daetz, R., Basso, F., Romero, J. J., *et al*. (2018).
571 Effects of homolactic bacterial inoculant on the performance of lactating dairy cows.
572 *Journal of Dairy Science, 101*(6), 5145-5152.

De Sitter, K., Garcia-Gonzalez, L., Matassa, C., Bertin, L., & De Wever, H. (2018). The use of membrane based reactive extraction for the recovery of carboxylic acids from thin stillage. *Separation and Purification Technology, 206*, 177-185.

Debergh, P., & Van Dael, M. (2022). Production of caproic acid from acetate and ethanol through microbial chain elongation: A techno-economic assessment. *Bioresource Technology Reports, 18*.

Every, D., & Ross, M. (1996). The role of dextrins in the stickiness of bread crumb made from pre-harvest sprouted wheat or flour containing exogenous alpha-amylase. *Journal of Cereal Science, 23*(3), 247-256.

Gao, R. Y., Li, Q., Chai, H. Y., He, Y. C., Yang, Z. F., & Ma, C. L. (2023). Synthesis of 5-Hydroxymethyl-2-furfurylamine from Bread Waste via Two-Step Reaction. *Acs Sustainable Chemistry & Engineering, 11*(42), 15315-15327.

Gemeinhardt, K., Jeon, B. S., Ntihuga, J. N., Wang, H., Schlaiss, C., Lucas, T. N., *et al.* (2025). Toward industrial C8 production: oxygen intrusion drives renewable *n*-caprylate production from ethanol and acetate intermediate metabolite production. *Green Chemistry, 27*(11), 2931-2949.

Grootscholten, T. I. M., Strik, D. P. B. T. B., Steinbusch, K. J. J., Buisman, C. J. N., & Hamelers, H. V. M. (2014). Two-stage medium chain fatty acid (MCFA) production from municipal solid waste and ethanol. *Applied Energy, 116*, 223-229.

592 Guerra-Oliveira, P., Fernández-Peláez, J., Gallego, C., & Gómez, M. (2022). Effects of particle
593 size in wasted bread flour properties. *International Journal of Food Science and*
594 *Technology, 57*(8), 4782-4791.
595 Huo, W. Z., Hu, T., Shao, Y. C., Ye, R., Muhammad, A., & Lu, W. J. (2024). Enhanced food
596 waste chain elongation for caproate production: Role of inorganic carbon and
597 optimization strategies. *Resources Conservation and Recycling, 203*.
598 Jung, J. M., Kim, J. Y., Kim, J. H., Kim, S. M., Jung, S., Song, H., *et al*. (2022). Zero-waste
599 strategy by means of valorization of bread waste. *Journal of Cleaner Production, 365*.
600 Kim, B. C., Moon, C., Jeon, B. S., Angenent, L. T., Choi, Y., & Nam, K. (2021). Shaping a reactor
601 microbiome generating stable n-caproate productivity through Design-build-test-learn
602 approach. *Chemical Engineering Journal, 425*.
603 Kim, H., Kang, S., & Sang, B. I. (2022). Metabolic cascade of complex organic wastes to
604 medium-chain carboxylic acids: A review on the state-of-the-art multi-omics analysis
605 for anaerobic chain elongation pathways. *Bioresource Technology, 344*.
606 Klask, C. M., Kliem-Kuster, N., Molitor, B., & Angenent, L. T. (2020). Nitrate feed improves
607 growth and ethanol production of *Clostridium ljungdahlii* with CO_2 and H_2, but results
608 in stochastic inhibition events. *Frontiers in Microbiology, 11*, 724.
609 Kucek, L. A., Spirito, C. M., & Angenent, L. T. (2016). High *n*-caprylate productivities and
610 specificities from dilute ethanol and acetate: chain elongation with microbiomes to
611 upgrade products from syngas fermentation. *Energy & Environmental Science, 9*(11),
612 3482-3494.

613 Kumar, V., Brancoli, P., Narisetty, V., Wallace, S., Charalampopoulos, D., Dubey, B. K., *et al.*
614 (2023). Bread waste - A potential feedstock for sustainable circular biorefineries.
615 *Bioresource Technology, 369*.
616 Li, X., Lei, X. L., Guo, Z. C., Yan, Z. Y., Gu, X., Xu, X. B., *et al.* (2024). Enhancing chain-
617 elongating microbiomes: Sequential fungi-bacteria cooperation for efficient food waste
618 upgrading using endogenous electron donors. *Chemical Engineering Journal, 488*.
619 Narisetty, V., Zhang, L., Zhang, J. X., Lin, C. S. K., Tong, Y. W., Show, P. L., *et al.* (2022).
620 Fermentative production of 2,3-Butanediol using bread waste - A green approach for
621 sustainable management of food waste. *Bioresource Technology, 358*.
622 Nzeteu, C. O., Trego, A. C., Abram, F., & O'Flaherty, V. (2018). Reproducible, high-yielding,
623 biological caproate production from food waste using a single-phase anaerobic reactor
624 system. *Biotechnology for Biofuels, 11*.
625 Nzeteu, C. O., Coelho, F., Trego, A. C., Abram, F., Ramiro-Garcia, J., Paulo, L., *et al.* (2022).
626 Development of an enhanced chain elongation process for caproic acid production
627 from waste-derived lactic acid and butyric acid. *Journal of Cleaner Production, 338*.
628 Palomo-Briones, R., Xu, J. J., Spirito, C. M., Usack, J. G., Trondsen, L. H., Guzman, J. J. L., *et*
629 *al.* (2022). Near-neutral pH increased *n*-caprylate production in a microbiome with
630 product inhibition of methanogenesis. *Chemical Engineering Journal, 446*.
631 Quintela, C., Grimalt-Alemany, A., Modin, O., Nygård, Y., Olsson, L., Skiadas, I., *et al.* (2024).
632 Effect of pH in syngas conversion to C4 & C6 acids in mixed-culture trickle bed
633 reactors. *Biomass & Bioenergy, 187*.

Rajagopalan, S., Datar, R. P., & Lewis, R. S. (2002). Formation of ethanol from carbon monoxide *via* a new microbial catalyst. *Biomass & Bioenergy, 23*(6), 487-493.

Roghair, M., Strik, D. P. B. T. B., Steinbusch, K. J. J., Weusthuis, R. A., Bruins, M. E., & Buisman, C. J. N. (2016). Granular sludge formation and characterization in a chain elongation process. *Process Biochemistry, 51*(10), 1594-1598.

Schuetterle, D. M., Hegner, R., Temovska, M., Ortiz-Ardila, A. E., & Angenent, L. T. (2024). Exclusive D-lactate-isomer production during a reactor-microbiome conversion of lactose-rich waste by controlling pH and temperature. *Water Research, 250*.

Spirito, C. M., Marzilli, A. M., & Angenent, L. T. (2018). Higher substrate ratios of ethanol to acetate steered chain elongation toward *n*-caprylate in a bioreactor with product extraction. *Environmental Science & Technology, 52*(22), 13438-13447.

Steinbusch, K. J. J., Hamelers, H. V. M., Plugge, C. M., & Buisman, C. J. N. (2011). Biological formation of caproate and caprylate from acetate: fuel and chemical production from low grade biomass. *Energy & Environmental Science, 4*(1), 216-224.

Swetha, T. A., Ananthi, V., Bora, A., Sengottuvelan, N., Ponnuchamy, K., Muthusamy, G., *et al*. (2023). A review on biodegradable polylactic acid (PLA) production from fermentative food waste- Its applications and degradation. *International Journal of Biological Macromolecules, 234*.

Teobaldi, A. G., Barrera, G. N., & Ribotta, P. D. (2024). Effect of damaged starch and wheat-bran arabinoxylans on wheat starch and wheat starch-gluten systems. *Foods, 13*(5).

654 Thani, N. M., Kamal, S. M. M., Taip, F. S., Sulaiman, A., & Omar, R. (2021). Sugar recovery
655 from bakery leftovers through enzymatic hydrolysis: Effect of process conditions and
656 product characterization. *Sains Malaysiana, 50*(10), 2977-2991.
657 Vasudevan, D., Richter, H., & Angenent, L. T. (2014). Upgrading dilute ethanol from syngas
658 fermentation to *n*-caproate with reactor microbiomes. *Bioresource Technology, 151*,
659 378-382.
660 Wang, J. L., & Yin, Y. A. (2022). Biological production of medium-chain carboxylates through
661 chain elongation: An overview. *Biotechnology Advances, 55*.
662 Weimer, P. J., & Kohn, R. A. (2016). Impacts of ruminal microorganisms on the production of
663 fuels: how can we intercede from the outside? (vol 100, pg 3389, 2016). *Applied*
664 *Microbiology and Biotechnology, 100*(8), 3399-3399.
665 Wu, Q. L., Bao, X., Guo, W. Q., Wang, B., Li, Y. X., Luo, H. C., *et al*. (2019). Medium chain
666 carboxylic acids production from waste biomass: Current advances and perspectives.
667 *Biotechnology Advances, 37*(5), 599-615.
668 Wu, Q. L., Feng, X. C., Guo, W. Q., Bao, X., & Ren, N. Q. (2020). Long-term medium chain
669 carboxylic acids production from liquor-making wastewater: Parameters optimization
670 and toxicity mitigation. *Chemical Engineering Journal, 388*.
671 Xu, J. J., Hao, J. X., Guzman, J. J. L., Spirito, C. M., Harroff, L. A., & Angenent, L. T. (2018).
672 Temperature-phased conversion of acid whey waste into medium-chain carboxylic
673 acids *via* lactic acid: No external e-donor. *Joule, 2*(2), 280-295.

Xu, J. J., Hao, J. X., Guzman, J. J. L., Spirito, C. M., Harroff, L. A., & Angenent, L. T. (2019). Temperature-phased conversion of acid whey waste into medium-chain carboxylic acids *via* lactic acid: No external e-donor (vol 2, pg 280, 2018). *Joule, 3*(3), 885-888.